Moisture content prediction of rain-exposed wood: Test and evaluation of a simple numerical model for durability applications

Niklewski, Jonas; Fredriksson, Maria; Isaksson, Tord

Published in:
Building and Environment

DOI:
10.1016/j.buildenv.2015.11.037

2016

For the complete, peer-reviewed version
doi:10.1016/j.buildenv.2015.11.037

Moisture content prediction of rain-exposed wood: Test and evaluation of a simple numerical model for durability applications

Authors: J. Niklewski[a], M. Fredriksson[b], T. Isaksson[c]

[a] Division of Structural Engineering, Lund University, PO-Box 118, SE-221 00 Lund, Sweden, +46462220330, jonas.niklewski@kstr.lth.se, Corresponding author

[b] Division of Building Materials, Lund University, PO-Box 118, SE-221 00 Lund, Sweden, +46 46 2227412, maria.fredriksson@byggtek.lth.se

[c] Skanska Sverige AB, Skanska Teknik, SE-205 33 Malmö, Sweden, +46 104481259, tord.isaksson@skanska.se

Abstract

Decay prediction models are frequently used to estimate the service life of wooden components. These models require knowledge of how the material climate, i.e. moisture content and material temperature, varies over time. Therefore, a reliable material climate prediction model is crucial in situations when measurements are not viable. The aim of this paper is to test and evaluate the performance of a simple numerical moisture transport model for rain-exposed wood. The main focus is on the influence of rain and moisture transport in the transversal direction.

First, a model based on Fick's second law of diffusion was calibrated against laboratory measurements where wooden boards were exposed to artificial rain. Second, the model was tested against field-test measurements on wooden boards in use-class 3.1, i.e. above-ground, exposed to rain and free to dry. The influence of rain was investigated by studying the difference between sheltered and exposed specimens over time. Finally, the model was applied to a number of Swedish climates and two different decay-prediction models were used to assess the output.

The main conclusion is that the influence of rain can be reproduced with sufficient accuracy for the particular application. The error between the numerical result and measurements tends to increase with decreasing temperature and at high moisture contents. However, the total error is reduced when the moisture content history is post-processed in a decay-prediction model as the rate of decay tends to decrease with decreasing temperature.

Keywords: moisture content, decay prediction, wood, durability

1 Introduction

As a building material, wood offers several advantages with respect to durability. Due to its natural insusceptibility to corrosion, the material has the potential to outperform both reinforced concrete and structural steel in outdoor applications. Moreover, provided that adverse chemical impregnation can be avoided, the material has a low environmental impact. On the other hand, in poor conditions the material degrades quickly due to fungal decay. So far, the guidance in the building codes is limited with respect to durability and service life of wood. For example, Eurocode [1] specifies that the effect of weathering should be taken into account and provides some general guidance for increased durability e.g. to avoid standing water and direct absorption between materials. However, no method to verify a target service life is given. Another example is the Swedish bridge standard, TRVK 11 [2], which specifies a minimum required level of structural protection and chemical impregnation based on the type of structure, required service life and use class. Although this type of prescriptive design format is practical, it fails to address several important decay-influencing factors such as the local climate.

A performance-based assessment based on the structure's actual climatic conditions would improve the designer's ability to make informed decisions with respect to durability design. The performance-based concept has previously been used to develop models for wooden decking and cladding where factors such as climate parameters, structural design and material properties were included [3]. A material climate prediction model can be used to link the external factors (e.g. climate and design) to the material climate which is expressed in terms of moisture content and temperature or alternatively relative humidity and temperature. Prediction models for the onset and rate of decay [4, 5] then link the material climate to a service life based on the resistance of the material. In existing structures, input to such models can be obtained from measurements. In design situations, on the other hand, the decay models are feasible only if the input can be expressed as functions of parameters available in the design phase, i.e. external factors such as weather. Therefore, an accurate climate prediction model is a key when designing for durability and estimating the service life of any timber structure.

Empirical functions of weather parameters are often used to predict material climate when estimating the service life of timber [6-8]. However, empirical models are not always related to actual material properties. Consequently, they are often limited to the type of wood and the specific depth for which the model was derived. Moreover, the influence of rain is difficult to include in a multiple regression model due to the time-lag between exposure and subsequent increase in moisture content [9].

Numerical models to predict material climate in timber are often subject to limitations in terms of moisture range and boundary conditions. Models based on Fick's second law of diffusion are frequently used in applications such as prediction of creep [10-12] and calculation of moisture induced stresses [13, 14]. However, the parameters of these models are usually limited to moisture contents below the fiber saturation point where wood is not susceptible to decay [4]. Moreover, moisture transport in the higher moisture range cannot solely be described as a diffusive phenomenon [15, 16], although it is sometimes used as a tool for approximation.

The main aim of the present study is to test and evaluate a simple numerical moisture transport model based on Fick's second law of diffusion which can provide input to decay prediction models when assessing the durability of rain-exposed wood. The scope is limited to timber in use-class 3.1 situations as defined by SS-EN 335 [17], i.e. above-ground, exposed to rain and free to dry. Moreover, the model is only tested for plane horizontal non-end grain rain-exposed surfaces. Exposure to rain is considered by imposing a fictive boundary moisture content during rain events. The results of the present study

are intended to be used together with subsequent research to produce a general moisture exposure model, including joints, for timber bridge applications.

The present study was carried out in three steps: calibration, verification and application of the model. In a first step (section 3) a numerical model based on Fick's second law of diffusion was calibrated against high-resolution data from a previous study on rain-exposed wood joints by Fredriksson *et al.* [18]. The model was then tested (section 4) in a use-class 3.1 situation by running it against field-test data presented by Isaksson and Thelandersson [3]. Special emphasis was put on the influence of rain by studying the difference between rain-exposed and a sheltered boards. In the final step (section 5) the model was applied to a number of typical Nordic climates. In the section 4 and 5 the material climate output was post-processed in decay-models and analyzed mainly in terms of decay rates.

2 Material and methods

2.1 Numerical model

The numerical model is based on Fick's second law of diffusion. In the one-dimensional case it may be written as:

$$dw/dt = d/dx(D\ dw/dx) \tag{1}$$

where the effective diffusion coefficient, *D*, and the gradient of moisture concentration, *dw/dx*, describes the net flow of moisture, *dw/dt*, within the material. The diffusion coefficient has been shown to depend on both moisture content and temperature [19]. The moisture exchange with the ambient air which occurs on the surface can be described as follows [14]:

$$q = S(w_{eq} - w) \tag{2}$$

where the surface flux, *q*, is a function of the surface transfer coefficient, *S*, and the difference between the boundary moisture concentration, *w*, and the equilibrium moisture concentration, w_{eq}, where the latter quantity is calculated from the sorption isotherm for the material. The surface transfer coefficient increases with increasing air velocity and decreasing temperature [20].

Previous research has reported discrepancies between models based on equations (1) and (2) and measurements [21]. These anomalies have led to the development of more complex multi-phase models [22, 23] which can be used in the hygroscopic range with higher accuracy than the single-phase models. However, the accuracy of the simple single-phase diffusion model is still sufficient for many engineering applications and has been shown to comply reasonably well with measurements in the hygroscopic range [24].

The diffusion coefficient can be described as follows [25]:

$$D(u,T) = D(u)\lambda(T) \tag{3}$$

where *u [kg/kg]* is the moisture content and *T* is the temperature in Kelvin. The moisture content related to the moisture concentration, *w [kg/m³]*, by the density of the material. In the hygroscopic range the rate of diffusion is commonly assumed to increase with increasing moisture content as well as temperature. For moisture contents higher than approximately 20%, the rate of diffusion decreases rapidly with increasing moisture content [26]. The temperature dependency can be assumed to follow an Arrhenius-type expression [25]:

$$\lambda(T) = C_1 \exp(C_2/T) \tag{4}$$

where C_2 is a coefficient that is common for many species of wood, T is the temperature in Kelvin and C_1 is chosen so that $\lambda(T)$ equals 1 at the calibration temperature which was 20˚C.

2.2 Model parameters

The material parameters include an effective diffusion coefficient, surface transfer coefficient, sorption isotherm and density. Moreover, when the surface is exposed to free water a fictive moisture concentration is imposed on the boundary. The effective diffusion coefficient governs the transport within the material while the surface transfer coefficient, sorption isotherm and fictive moisture concentration govern the boundary conditions.

2.2.1 Parameters

In the present study the diffusion and surface transfer coefficients were taken from literature. However, the literature offers a wide range of values for both coefficients [27, 28]. Therefore, several different coefficients were tested against the experimental data in [18] and the set of coefficients which produced the best fit was selected. To address the variability/uncertainty related to the diffusion coefficient, two different diffusion coefficients from [27] were selected (see Figure 1) and used throughout the present study. The surface transfer coefficient was taken from [29].

The constant governing the temperature-dependency of the effective diffusion coefficient, C_2, was taken from [25]. Knowing the temperature at which the effective diffusion coefficient was experimentally determined (293 K), C_1 was calculated from equation (4) using the condition $\lambda(293) = 1$. The temperature-dependency is illustrated in Figure 2.

The sorption isotherm is shown in Figure 3. The function was calculated as the average of four Hailwood-Horrobin-type absorption isotherms presented in [30]. Note that the function is extrapolated for values above 97% relative humidity and does not resemble the steep increase which is known to occur at high relative humidity. Moreover, the influence of hysteresis was not included in the model.

The fictive boundary moisture concentration during wetting, w_{wet}, was used as a fitting parameter and was calibrated against the data in [18]. The value does not necessarily represent the actual moisture concentration on the surface but is used as a simplified way of describing the otherwise complex boundary condition during wetting.

All material parameters are compiled in Table 1.

2.2.2 Dose-model

A dose model predicts material degradation over time as a cumulative damage function, similar to that of Miner's rule [31] which is used in fatigue applications. Doses are accumulated at a rate which is determined based on the material climate, the maximum being one dose per day which represents perfect conditions for decay. The daily dose at day i, d_i, is a function of two components: the temperature induced dose, d_T, and the moisture induced dose d_u, calculated from the daily average temperature, $\overline{T}$, and the daily average moisture content, $\overline{u}$, respectively. Both components are required to be above zero for a dose to be produced. The total dose is the cumulative sum of daily doses from day 1 to n according to:

$$d = \sum_{i=1}^{n} d_i(d_u(\overline{u}), d_T(\overline{T})) \qquad (5)$$

Failure of the component occurs when the accumulated dose, d, reaches a limit state, d_{crit} and the service life is defined by the corresponding amount of days, n, until the limit state is reached. The limit

state is defined by the dose which corresponds to a certain level of decay. Two different dose models were used here, both described in [32].

The main difference between the models is the relation between daily average moisture content and moisture induced dose, i.e. the relation between $\bar{u}$ to d_u. The so called *logistic model* uses a lower threshold of 25% moisture content, below which no moisture induced dose is produced. Therefore, wood which sustains a moisture content below 25% never reaches the limit state. This assumption is supported by most research. Conversely, the *simplified logistic model* does not define any moisture content threshold. The logic is that the model takes different types of uncertainties into account and that relative exposure levels can be estimated also for data sets where the moisture content is mainly below 25%. A detailed description of the models and its governing equations can be found in [32].

In sections 4 and 5 the model output is post-processed using these decay prediction models. In section 4 the conversion from material climate to dose was performed using only the simplified logistic model. In section 5 the logistic model was used in addition to the simplified logistic model.

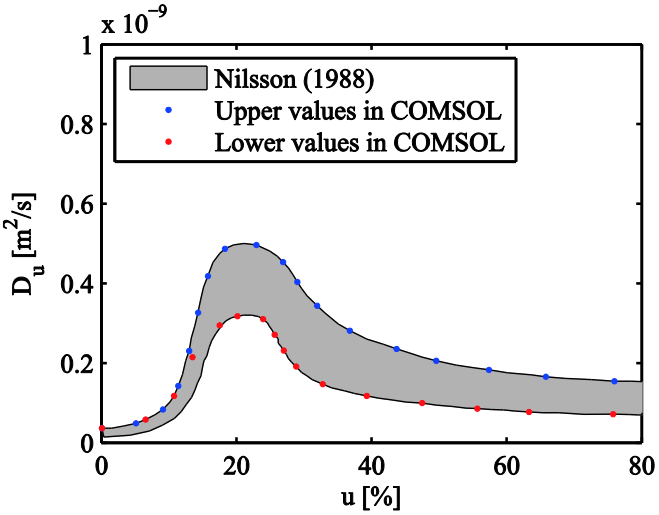

Figure 1 – Diffusion coefficient. Range from literature (gray), together with the upper (blue) and lower (red) values implemented into COMSOL.

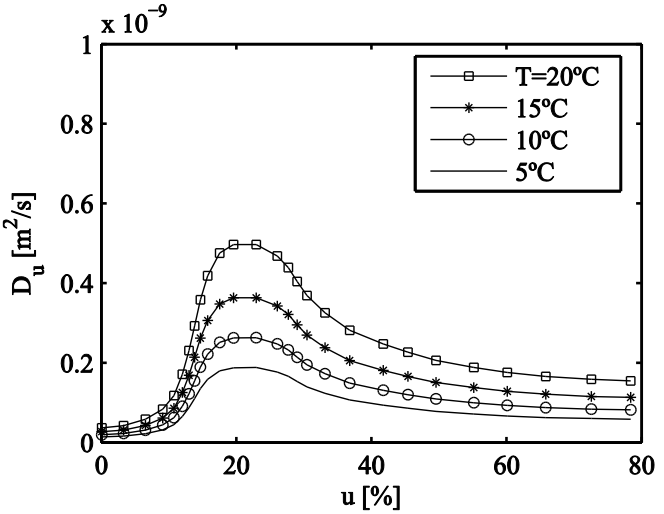

Figure 2 – Diffusion coefficient (only upper values) at various temperatures.

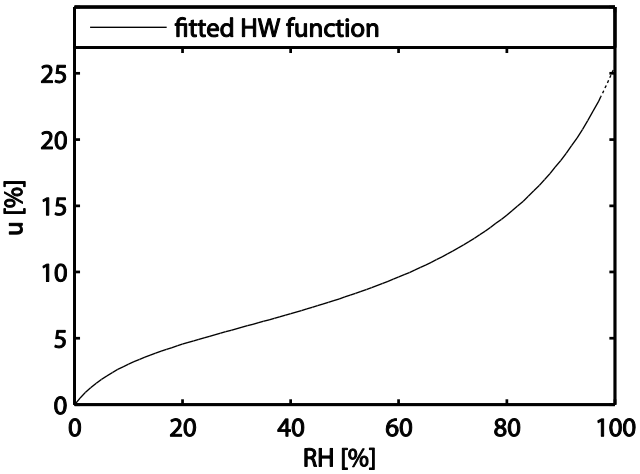

Figure 3 – Absorption isotherm. Measured values and fitted function as implemented in COMSOL. The upper part of the sorption isotherm (>97% RH) is extrapolated.

Table 1 – Summary of material properties.

Property	Value	Reference
Boundary moisture content, w_{wet}	See section 3.2.1	
Surface transfer coefficient, S	$1.4*10^{-7}$ m/s	[29]
Density, ρ	345 kg/m^3	[33]
Temperature dependency		
C_1	$6.7*10^7$	Derived from eq. (4)
C_2	-5280	[25]
Sorption isotherm[1]		HW coefficients A-C were fitted from data in
A	1.897	[30]
B	$1.150*10^{-1}$	
C	$1.301*10^{-3}$	

[1] *Hailwood-Horrobin equation:* $u=\varphi \cdot (A + B\varphi - C\varphi^2)^{-1}$

2.3 Implementation into COMSOL

A one-dimensional finite element model based on equations (1) and (2) was developed in the commercial software COMSOL Multiphysics [34] using the coefficient form Partial Differential Equation (PDE) interface. The moisture flux in the domain as well as on the boundary was governed by the following equations:

$$dw/dt - d/dx\,(D\,dw/dx) = 0 \qquad in\ the\ domain \qquad (6)$$

$$q = S(w_{eq} - w) \qquad on\ the\ boundary\ (no\ rain) \qquad (7)$$

$$w = w_{wet} \qquad on\ the\ boundary\ (during\ rain) \qquad (8)$$

For simplicity, both boundary conditions were implemented as Neumann-type boundary conditions, i.e. boundary moisture fluxes on the same form as equation (7). By assigning a large value to the surface transfer coefficient and changing w_{eq} *for* w_{wet}, the Neumann-type condition becomes analogous to the condition given by equation (8). It should be noted that (8) applies exclusively to boundaries which are exposed to rain. For example, rain-exposed boundaries switch from (7) to (8) when the rain starts and switch back instantly when rain stops. The model is calibrated for measurements on rain-exposed horizontal surfaces thus a short period of standing water is implicitly included in the fitted parameter.

The longitudinal as well as the lateral moisture gradients were neglected and thus a one-dimensional slab model could be used. The geometry was defined by the thickness of the boards, i.e. 22 mm in all cases. The material parameters were taken from Table 1.

3 Calibration

3.1 Input and data

In an experiment on rain exposed wood joints presented by Fredriksson *et al.* [18], the moisture content profiles in three types of joints, each with different gap-sizes (0, 2 and 5 mm), were monitored continuously during and after exposure to artificial rain. Both fast grown and slow grown Norway spruce *(Picea abies)* were used. Two different exposure situations were included. Initially, all specimens were conditioned to a relative humidity close to the climate in the room (65% RH/20˚C) in which the experiments were performed. The specimens were exposed to 6,5 hours of rain and moisture content profiles were monitored both during wetting and the subsequent drying in 65%

RH/20˚C, see [18]. Secondly, the same specimens were exposed to cyclic rain events; one hour of rain every 24-hours during five days [35]. A detailed description of the experimental setup is found in [18]

Three points of measurements in end-grain to side-grain T-joints were used for calibration. Since the influence of a joint or a moisture trap was not included in the present study, the point of measurements furthest away from the joint was chosen for calibration of the model. The points of measurements used for calibration were located in the horizontal board (590x22x95mm^3) at three depths (3, 11 and 19 mm) in a cross-section 20 mm from the joint, see Figure 4. The edges of the specimens were sealed so that only the upper surface of the horizontal board was exposed to rain. The boundary conditions on the different surfaces were thus well-defined. Due to the relatively large distance from the moisture trap, the longitudinal moisture gradient was small, thus longitudinal moisture transport was neglected and a one-dimensional analysis was used. This was also the reason why points of measurements in the horizontal board were chosen; in the vertical board the points of measurements were close to an end grain surface and thus the longitudinal moisture transport dominated. Provided that the longitudinal transport was negligible, any difference between the three data sets can likely be attributed variations of material response.

In the numerical model the temperature was assumed to be constant at 20˚C and the ambient relative humidity was implemented from measured data. The duration of rain was well-documented and could be implemented directly as a step-wise function of time (Figure 5). During any sequence of rain it was assumed that the relative humidity increased to 100%. However, this assumption mainly influenced the non-rain-exposed surface. The initial moisture content was assumed to be uniformly distributed and in equilibrium with the absorption isotherm at 65% relative humidity. This yields an initial moisture content of approximately 10.5% which is close to the measured value right after conditioning. The same initial condition was used for both exposure situations. The calculation was performed for values of w_{wet} ranging between 240 and 500 kg/m^3.

The measured initial moisture content varied between test specimens as well as between exposure situations. The difference *between test specimens* is likely related to material variability/measurement precision whereas the difference *between exposure situations* is related to hysteresis. To be able to simultaneously compare all measured data to a single simulation (per exposure situation), the change of moisture content, $\Delta u_{t,j}$, rather than the moisture content variation is studied. This is done by deducting the initial moisture content, $u_{t=0,j}$, from each time-step and in each point of measurement, j, according to equation (9).

$$\Delta u_{t,j} = u_{t,j} - u_{i,j} \qquad (9)$$

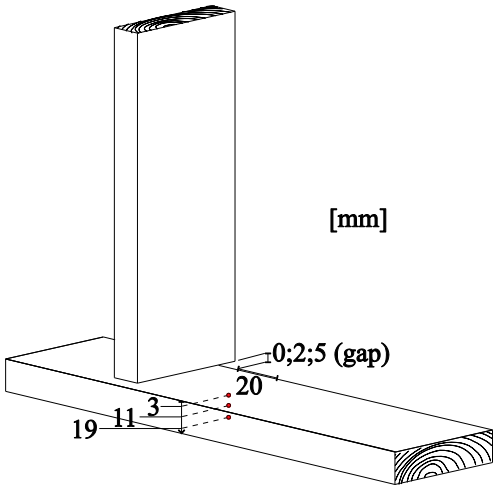

Figure 4 – Schematic illustration of the test setup.

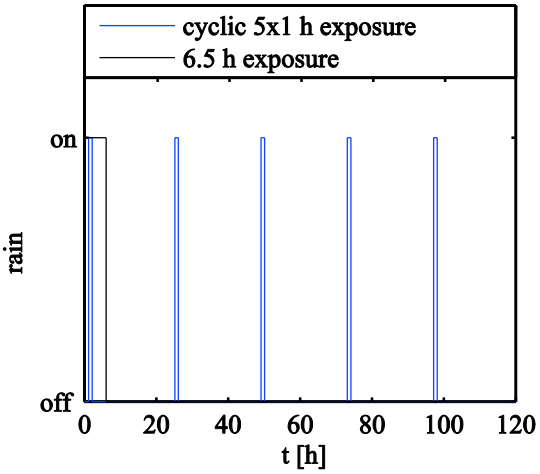

Figure 5 - Rain history as implemented in COMSOL.

3.2 Results and discussion

3.2.1 Calibration parameter, w_{wet}

The measured data plotted against the numerical solution at each depth (3, 11 and 19 mm) for the two exposure situations are presented in Figure 6. The numerical solution was obtained using w_{wet}*=345 kg/m*^{3} which corresponds to a moisture content of u=100%. The value was determined based on a qualitative evaluation of a large number of simulations where the calibration parameter, w_{wet}, was varied in the range of 240-500 kg/m^3. The determined value is used in the continuation of the present study.

3.2.2 Variability of test specimens

The varying test results within the fast-grown subgroup indicate that there is a significant variability, with respect to permeability, between individual specimens. The fact that the variability is less pronounced between slow-grown specimens indicates that it may be related to the number of growth rings per specimen. There are two possible explanations to this higher variability for the specimens of fast grown wood. First, the width of the growth rings in the fast grown wood was so large so that it is likely that the moisture content was measured either in the latewood or in the earlywood which could result in significant differences between specimens. However, for the slow grown wood, the growth rings were so thin that the measured moisture content was a combination of the moisture content of the earlywood and the latewood. The difference between individual specimens due to this aspect

should thus be smaller for the slow grown wood. Secondly, since there is a difference in permeability between earlywood and latewood [36], the moisture content at a certain depth is dependent on in which order the growth rings are arranged, for example if the growth ring closest to the surface is earlywood or latewood. However, this has only an influence when there are a small number of growth rings per specimen.

Due to the variability described in the previous paragraph, the model cannot be assessed from the long-exposure test data alone. However, for both exposure situations it is seen that the measured data and the numerical solution are in good agreement with respect to the time until peaking moisture content as well as drying rate. Moreover, during cyclic exposure the model predicts also the change of moisture content with sufficient accuracy at all three depths.

3.2.3 Limitations

As seen in Figure 6a-c, the model fails to predict the equilibrium moisture content at the end of the first test. Failure to predict the equilibrium condition is a direct consequence of neglecting the influence of hysteresis. However, in most practical situations with varying relative humidity, the error related to hysteresis is small. Moreover, the error can be reduced by using the mean sorption isotherm, i.e. a curve located between the absorption and desorption isotherms. However, this was not done in the present study.

The biggest discrepancy between model and measurements can be seen in Figure 6a where the difference between the numerical result and the fast-grown specimens exceeds 20 percentage points (actual value is unknown) subsequent to the initial wetting. The large errors quickly diminishes and after six hours of drying, two out of three fast-grown specimen have reached moisture contents similar to the numerical solution. The large errors are likely related to the high moisture levels (u>40%) where the moisture transport cannot be described solely by diffusion. This is supported by the fact that the same type of error is not observed during the second test where the moisture content never exceeded 35%. A similar behavior can be found in experiments on wood drying [16] where the drying rate tends to level off around a threshold of 40% moisture content.

In durability application, decreased model accuracy at high moisture levels (u>40%) does not necessarily impair the quality of the decay prediction, provided that the time above fiber saturation is correct. The reason is that absolute values above the fiber saturation point are rarely used in decay prediction models. In fact, the simplified logistic model does not differentiate between moisture contents above the fiber saturation point, i.e. the moisture induced dose is constant above the fiber saturation point (see section 2.2.2). Moreover, since moisture contents above the fiber saturation point are difficult to measure with resistance-type moisture sensors, metrics such as the *time above 25% moisture content* are sometimes favored over absolute values. Therefore, it is reasonable to accept some deviation in terms of absolute moisture content in the higher moisture regions provided that the time above fiber saturation complies reasonably well with the data, which appears to be the case.

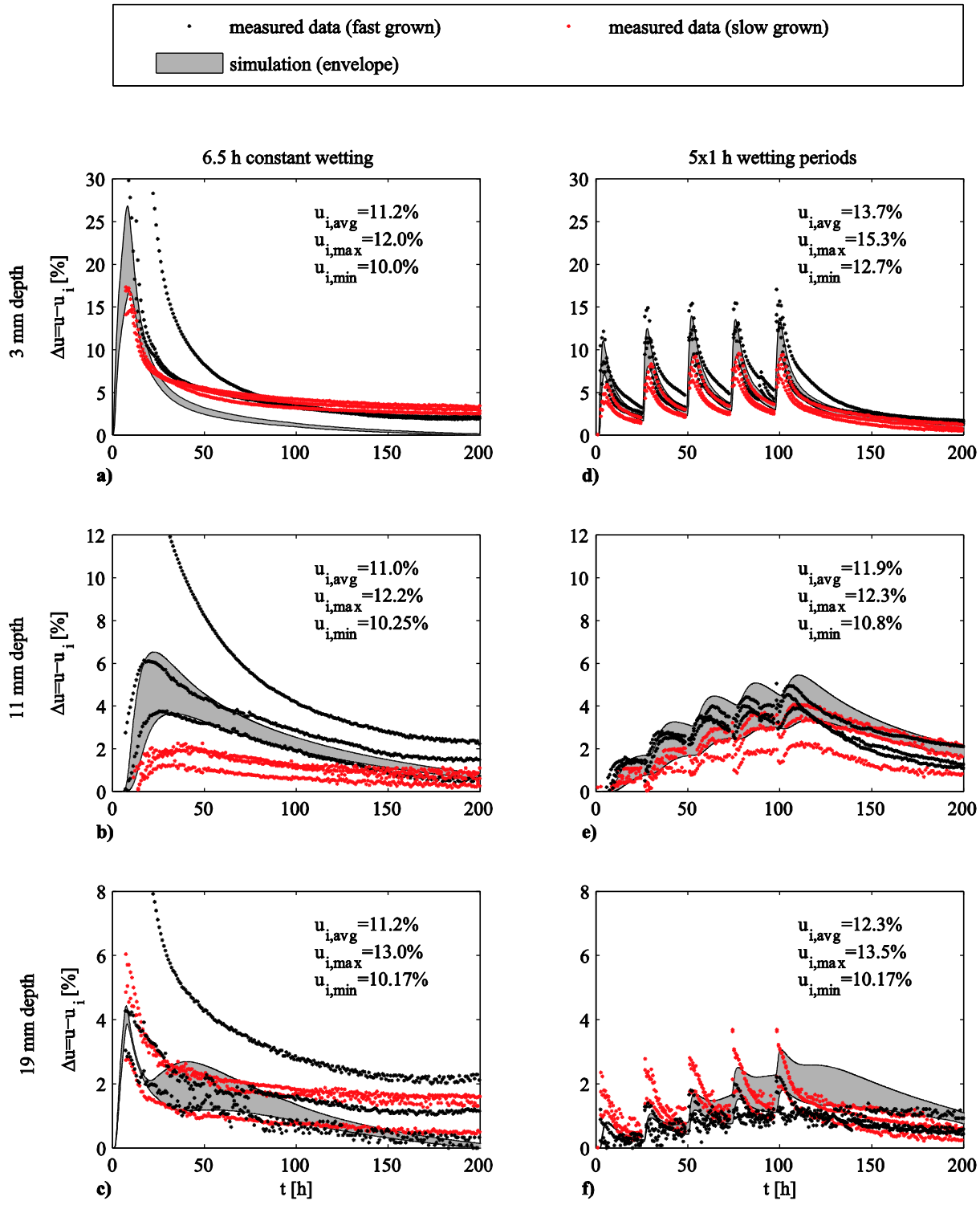

Figure 6 - Measured moisture content plotted together with numerical result at various depths (top to bottom) and for two different exposure conditions (left and right columns). The average, max and min initial (t=0) measured moisture content, u_i, is displayed in the graph. The calibration parameter, w_{wet}, was set to 345 kg/m^3.

4 Model verification

4.1 Input and data

The numerical model, calibrated as described in 3, was tested in a use-class 3.1 situation by running it against data from a field-test conducted by Isaksson and Thelandersson [3]. The data set includes two sets of Norway spruce *(Picea abies)* specimens (22x95x500mm^3) which were exposed outdoors for two years while relative humidity [%], temperature [˚C] and precipitation [mm/h] were recorded every ten minutes at the test site. Gaps in the time-series due to weather station outage were filled using alternative sources e.g.: SMHI [37].

The moisture content was measured continuously at a depth of 11 mm as well as on the surface using resistance-type moisture sensors. An expression from [38] was used to calculate the moisture content from the resistance and temperature. Since no calibration of the measurement system was performed, the moisture content output in terms of absolute values is inherently inaccurate. However, changes in moisture content as well as relative differences between specimens are measured with relatively high accuracy even without calibration. A detailed description of the test-setup can be found in Isaksson and Thelandersson [3] and the method which was used to measure surface moisture is described by Fredriksson *et al.* [39].

For consistency, the model was implemented strictly as described in section 3 and no parameters were altered. The input relative humidity is implemented as a time-series of hourly measured data using linear interpolation between sampling points. The material temperature is assumed uniformly distributed and equal to the air temperature. However, to account for some lag between the air and material temperature, the daily average temperature is used.

The duration of rain was estimated from the hourly data and was implemented as a step-wise function of time. Prior to implementation into COMSOL, the raw weather data required some pre-processing as the recorded unit, mm/h, was incompatible with the model which requires a duration (see section 2.3). In the present study it was assumed that any hour during which the amount of rain, p_{60}, exceeded a threshold of 2 mm corresponds to an uninterrupted 1-hour sequence of rain. Moreover, it was assumed that the intensity of low to intermediate rain events (p_{60}<2 mm) was constant, thus a linear relationship between accumulated precipitation and duration can be used. Following the two previous assumptions while assuming that the linear relation between duration and accumulated precipitation must pass through the origin, the duration of any rain event is calculated as follows:

$$t_{r,60} = \begin{cases} 30p_{60} & 0 < p_{60} < 2 \\ 60 & p_{60} \geq 2 \end{cases} \qquad (10)$$

where p_{60} [mm/h] is the hourly amount of rain and $t_{r,60}$ [min] is its corresponding duration. The underlying assumptions of equation (10) are based on a high-resolution data set (6 samples per hour) from the test-site including 2500 hours with recorded rain during a 3-year period.

4.2 Results and discussion

4.2.1 Absolute moisture content

The daily average moisture content at 11 mm depth, plotted over a period of one year is shown in Figure 7 for the numerical solution and the measurements respectively together with the rain history for the same period. Each exposure situation (exposed/sheltered) is represented by a range where the upper and lower bound differs only with respect to the diffusion coefficient. The measured data in Figure 7 represents the average of the two sheltered and the two exposed specimens respectively. However, in sections 4.2.1 and 4.2.2 the exposed specimens are treated separately (denoted specimen

A and B) as there appears to be a significant discrepancy between the two. The sheltered specimens are always treated as an average as the difference between the two is negligible. Although the specimens were monitored for two years, only the second year is used here as the weather history from the first year has not been quality-checked. However, the first and the second year display the same characteristics.

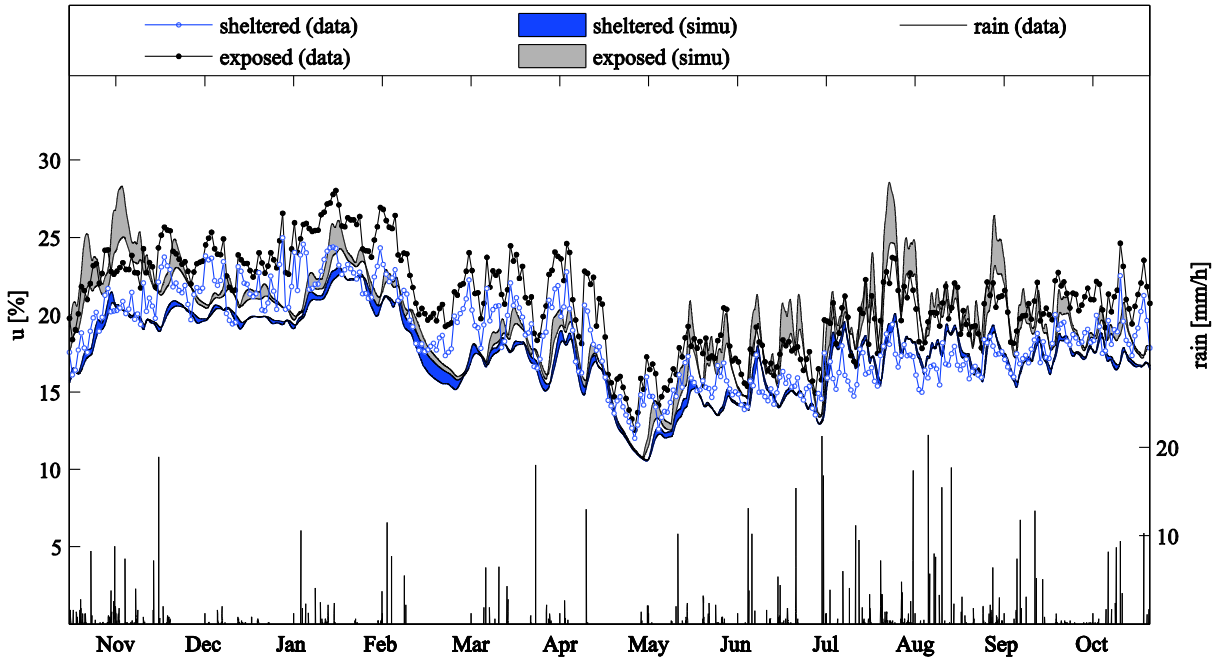

Figure 7 – Measured average moisture content of exposed specimens (black dots) and sheltered specimens (blue dots) plotted together with numerical solution including rain (gray envelope) and excluding rain (blue envelope). The time-period is from 20-Oct 2010 to 20-Oct 2011.

4.2.2 The influence of rain

The influence of rain is investigated by studying the difference in moisture content between the rain-exposed and the sheltered specimens. The absolute difference, Δu_{rain}, is defined as the difference in moisture content between the sheltered and the exposed specimen, $\Delta u_{rain} = u_{exp} - u_{shelt}$. Since the two sheltered specimens are treated as an average, only two time-series of Δu_{rain} are obtained, one for each exposed specimen. Days when the weather station was offline were excluded from this part of the analysis.

The cumulative distributions of the absolute differences, Δu_{rain}, are shown in Figure 8. The year has been separated in a warm (Figure 8a) and a cold (Figure 8b) season in order to study the effect of temperature on the performance of the model. The cumulative percent, on the vertical axis, indicates the portion of time during which the absolute difference, Δu_{rain}, is lower than a certain value. For example, during 90% of the days between April and October, the absolute difference between the sheltered board and specimen B is lower than 4 percentage points. The measurements indicate that the moisture content of specimen B was consistently higher than that of specimen A. This is either due to material variability, measurement error or a combination of the former. The fact that the difference diminishes with increasing moisture content is probably because the upper limit of the sensor (approximately 25%) is reached.

The model performs relatively well during the summer when the temperature is high (Figure 8a). For example, the lower bound solution is in very good agreement with the measurements taken from specimen A. However, the performance appears to decrease with decreasing temperature (Figure 8b). This is likely because the warm season (Figure 8b) better resembles the calibration temperature (20˚C)

which was used in section 3. Moreover, it is difficult to distinguish between snow and rain whereas the former has a minor influence on the moisture content. The model treats all precipitation as rain and therefore overestimates the moisture content during subfreezing temperatures. However, the fact that the model is less accurate in cold climate is not necessarily a problem in durability applications as the daily induced dose decreases with decreasing temperature. This effect is illustrated in Figure 9 which shows the cumulative distributions of difference in daily dose, ΔD, calculated according to the simplified logistic model. As can be seen in Figure 9b, during 50% of the cold period the difference is zero, the main reason being that the temperature is below zero and no dose is generated.

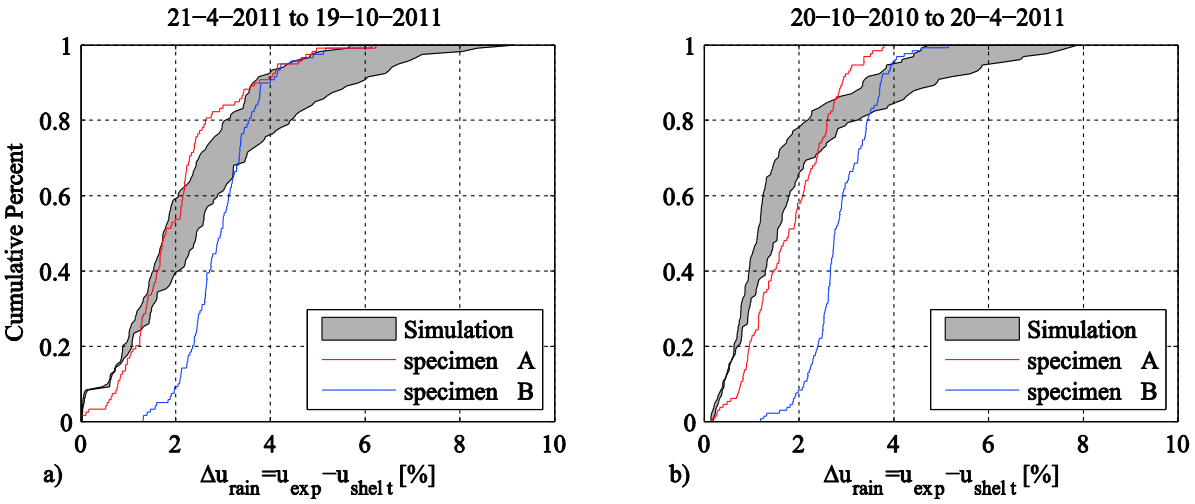

Figure 8 - Cumulative distribution of the absolute difference for the warm season (left) and the cold season (right).

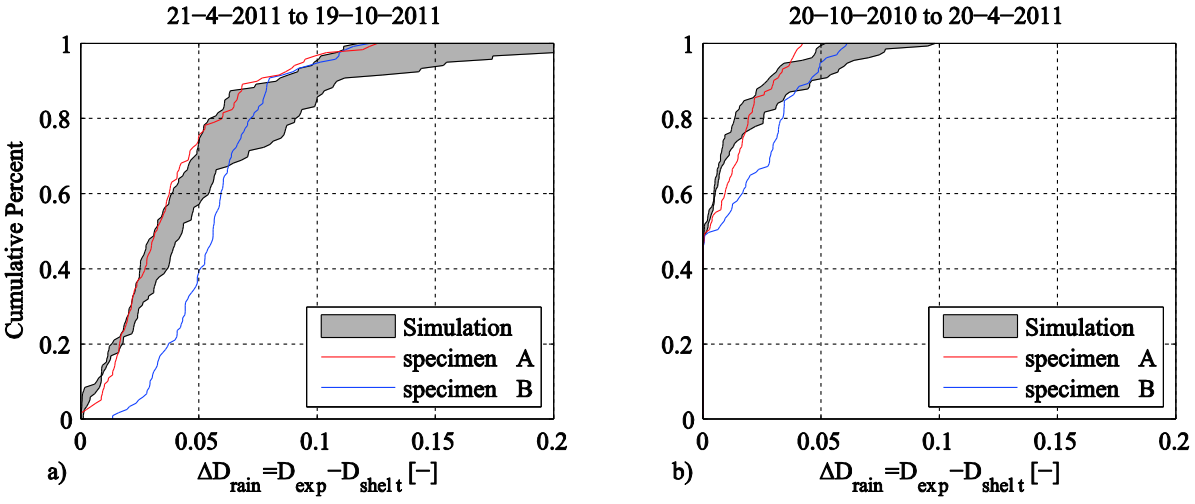

Figure 9 - Cumulative distribution of the difference in dose between sheltered and exposed specimens, plotted for the warm season (left) and the cold season (right) separately.

Figure 10 shows the daily average upper bound prediction plotted against the corresponding measured value. Pearson's product moment correlation coefficients, $\rho_{X,Y}$, between the numerical, Y, and the measured, X, absolute differences are 0.71 and 0.56 between April and October (Figure 10a) compared to 0.47 and 0.09 from October to April (Figure 10b). The correlation coefficient is a good complement

to the cumulative distribution as it provides information regarding the model compliance *in time* whereas the cumulative distribution compares the compliance *over a period of time*. Ideally, when using the correlation coefficient as a measure of agreement it should be equal to or close to 1. This is the reason why no significance test is included. Potential reasons for the overall poor correlation include both model and measurement inadequacy. For example, the worst correlation coefficient (0.09) can be explained by the fact that specimen B frequently exceeds the fiber saturation point during the cold period, above which the sensor output is very uncertain. Moreover, sometimes the model successfully reproduces a moisture content peak subsequent to a wet period but fails to predict the correct time-lag between the two. This of course results in poor correlation.

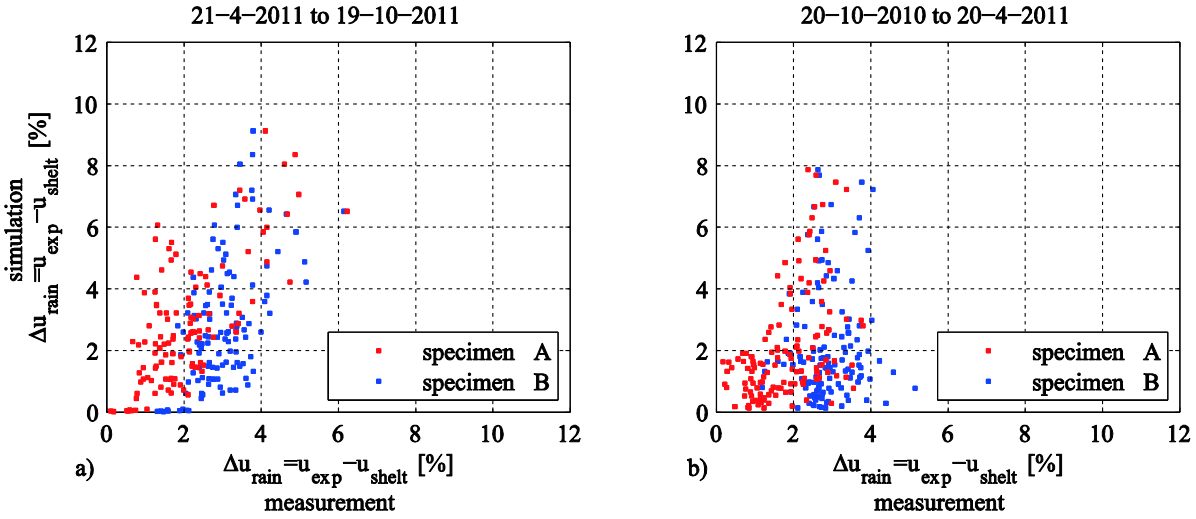

Figure 10 - Comparison between absolute difference in moisture content between sheltered and rain-exposed board plotted for the warm season (left) and the cold season (right).

4.2.3 Surface wetness

The compliance between real boundary condition and model input is studied by comparing the numerical result on the boundary with the surface sensor data. The surface sensor was designed from a resistance-type sensor with two electrodes enclosed in non-conductive capillary tubing, effectively separating the electrodes from the wood. Consequently, a dry surface was seen as the sensor's minimum output (8%). When the surface was completely wet, the two electrodes were connected by a water-film on the surface. As the resistance of water is magnitudes lower than that of wood, the output of the sensor peaked at 30-40%. Any value in-between these two extremes indicate that the water-film covered the capillary tubing but did not fully bridge the distance between two electrodes. This happened (1) when a water-film was drying and (2) with dew on the surface. As dew is related to the relative humidity of the air, small peaks in the output of the surface sensor coincided with high relative humidity.

Prior to the comparison it was advantageous to filter the two time-series. The filter used the partially periodic nature of the time-series to identify the non-periodic rain induced peaks using discrete Fourier transformation. The numerical solution was periodic due to its annual and daily relative humidity fluctuations whereas the surface sensor measurements were partially periodic due to the correlation between high relative humidity (night-time dew) and surface moisture. First, the two time-series were transformed to the frequency domain using MATLAB. While in the frequency domain, the amplitude of the daily frequency as well as the annual frequency were set to zero after which the time-series were transformed back to the time-domain. By removing the lower frequencies, both data series were effectively centered close to zero. By removing the daily frequencies, the peaks due to night-time dew

(measured data) and the daily moisture content variation (numerical results) were minimized. As a result the rain induced peaks became easier to identify. The same operation was performed on both time-series and the width of the rain induced peaks were not significantly altered by the filter. The data from the cold season was excluded as readings with ice and snow on the surface are impossible to distinguish from free water.

The filtered data can be seen in Figure 11 for a period of 500 hours during summer. To avoid confusion, the unit has been removed from the y-axis. Although the unit is unaffected by the filter, the filtered data no longer reflects the moisture content. It can be seen that the model in many cases successfully reproduces both the timing and the width of the measured peaks. However, in some cases the model produces a false peak or fails to produce one. These events almost always coincide with weather station outage. Any deficiency of equation (10) may lead to both overestimated and underestimated time of wetness depending on the intensity of the specific rain-event.

The cumulative time of wetness, ToW, was evaluated by defining an appropriate threshold which was exceeded by the filtered data only during peaking moisture content i.e. rain induced peaks. The cumulative time during which the threshold was exceeded was calculated from the measured data and the numerical solution on the boundary respectively. Using a threshold of 4%, the ToW increases with time as seen in Figure 11. The resemblance between the numerical results and measured data is consistent for thresholds ranging between 3-7% percentage points. The result indicates that the time during which the sensor registers rain on the surface correlates very well with the time during which the predicted moisture content remains high during as well as subsequent to rain events on the boundary.

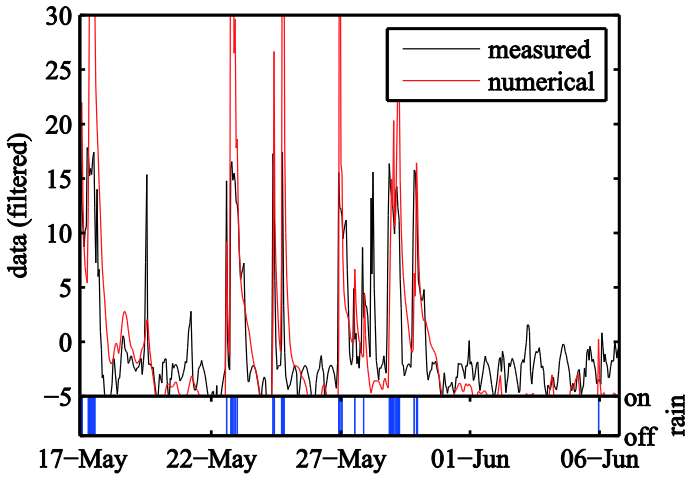

Figure 11 – Rescaled output from surface moisture sensors plotted together with rescaled numerical boundary moisture content. Duration of rain (from eq. (10)) is also included (bottom).

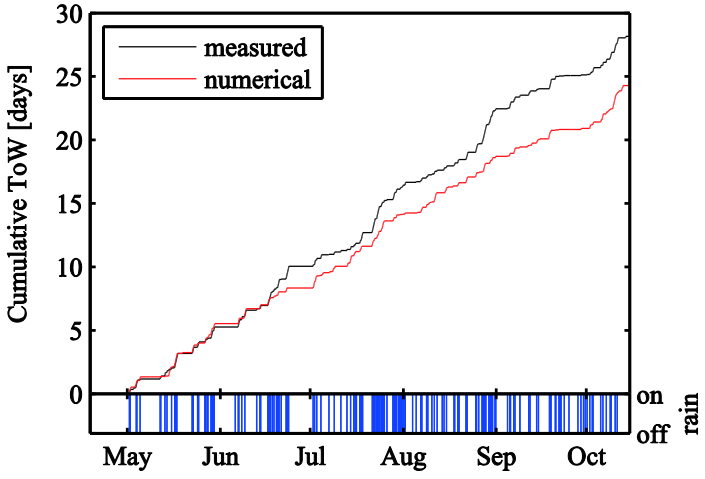

Figure 12 – Cumulative time of wetness, ToW, when the rescaled moisture content exceeds the 4% threshold. Duration of rain (from eq. (10)) is also included (bottom)

5 Estimated service life in Swedish climate

5.1 Input and data

The model from section 3 and 4 was used to calculate the estimated service life (ESL) for a wooden specimen (22 mm thick) located in 11 Swedish cities. First, the moisture content over time was calculated from one year of hourly climate data, including temperature [˚C], relative humidity [%] and precipitation [mm/h]. The data was obtained from the software Meteonorm [40] and each data set represents a Meteonorm normal year. Second, the moisture content output and the air temperature were used to calculate the spatial distribution of annual induced dose using two dose-response models as described in section 2.2.2. Finally, the annual dose was extrapolated until the limit state, as defined by decay rating 1 (onset of decay), was reached. This limit state corresponds to a dose of 452 for the logistic and 442 for the simplified logistic model.

5.2 Results and discussion

5.2.1 ESL dependence on depth

Figure 13 shows how the inverse of the calculated ESL varies with depth in a specimen located in Lund. The inverse is used to avoid values going towards infinity when the annual dose approaches zero. The simplified logistic model results in a shorter service life at any depth compared to the logistic model. At a depth of 10 mm, the dose equals zero according to the logistic model. The reason is that the moisture fluctuations are increasingly damped with depth, thus only the material close to the exposed surface frequently exceeds 25% moisture content i.e. the lower limit for decay growth according to the logistic model (see section 2.2.2). This type of moisture differential is one of the reasons why the simplified logistic model was developed [32]. Resistance-type moisture measurements are for practical reasons often taken at least 10 mm from the surface of the wood. Using the moisture history from this depth directly as input to the logistic model, without accounting for the damping effect, may impair the estimation and result in unrealistic service lives.

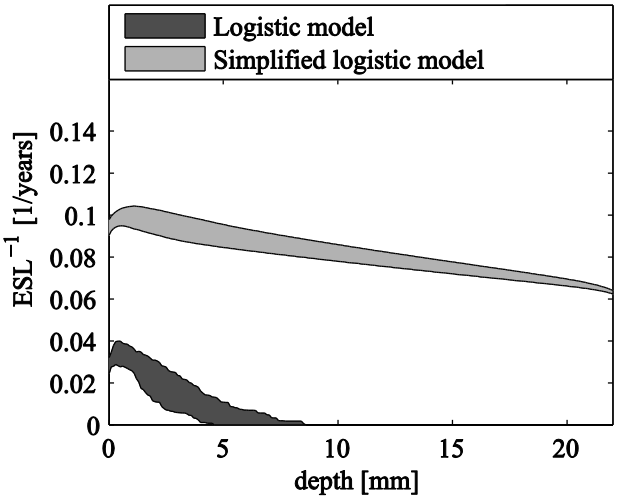

Figure 13 – Spatial distribution of the inverse of the estimated service life for a board located in Lund, calculated according to the simplified logistic model (light gray range) and the logistic model (dark gray range).

5.2.2 ESL dependence on climate

Figure 14 compiles the inverse of the estimated service lives of 11 specimens located in various Swedish cities. The ESL is taken from the "most severe depth" which is always close to the exposed surface. The cities are sorted in descending order based on latitude. Again, the simplified logistic model predicts lower service lives compared to the logistic model. The difference between the models varies with a factor of 2-3 depending on the location. The ratio between the highest and lowest ESL is approximately 2.5 for both models. Overall, the service life tends to decrease with decreasing latitude. This is mainly an effect of the increasing average temperature.

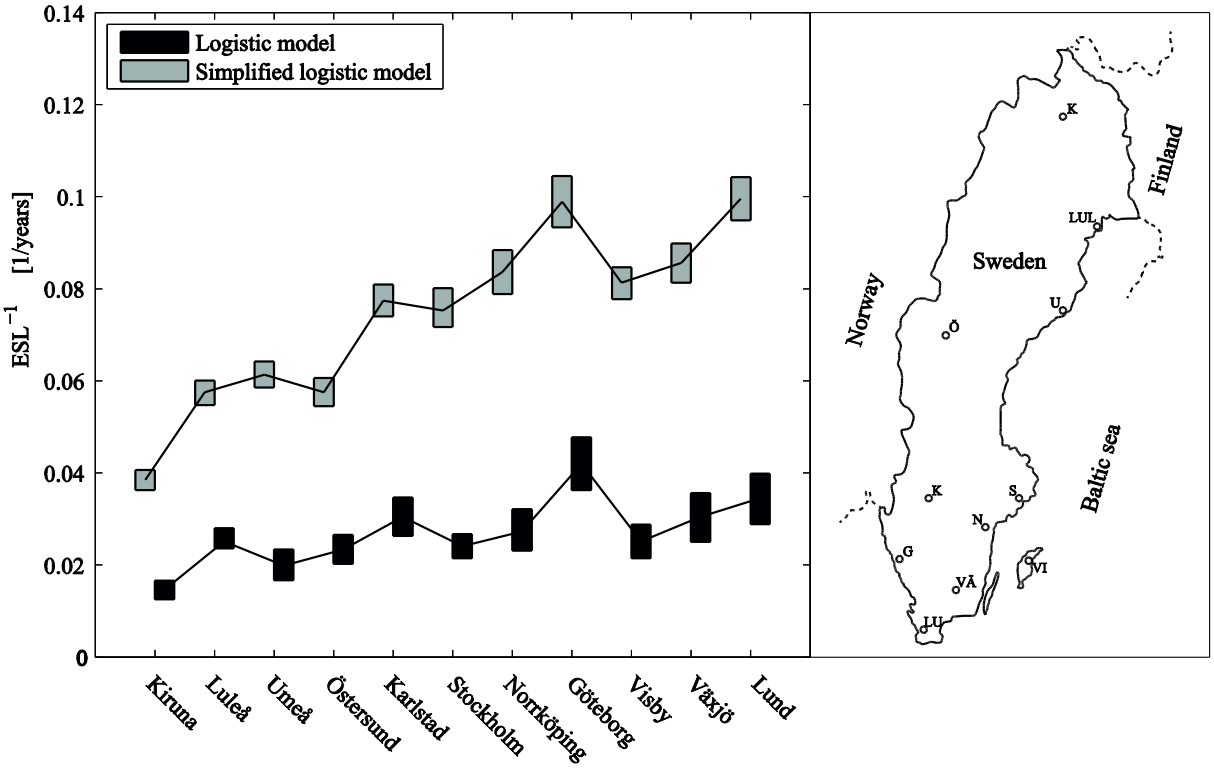

Figure 14 – Inverse of the estimated service lives calculated using the logistic (light gray) and the simplified logistic model (dark gray) at 11 different locations in Sweden. The calculations are based on the annual dose at the most severe depth with respect to decay. The map shows the location of the cities from which the weather data was taken.

6 Conclusions

A method to predict the moisture content of rain-exposed wood was tested and evaluated. A simple numerical model based on Fick's second law of diffusion with moisture concentration as the only driving force was used to predict the moisture content of rain-exposed wood based on the surrounding relative humidity, temperature and rain history. The model relies on a fictive boundary condition which imposes a fixed moisture concentration on the boundary during rain events.

It was found that the model can be used, with sufficient accuracy for durability applications, to study the moisture content of rain-exposed wood when moisture transport in the transversal direction is dominating. The model can, with reasonable accuracy, predict the moisture content during, as well as subsequent to, rain events of short to medium duration. Predicted values in the upper moisture region (e.g. close to the surface after a long sequence of rain) should be considered approximations since the absolute value becomes increasingly uncertain with increasing moisture content. However, the duration of high moisture content appears to be reasonably accurate, rendering the model suitable for decay prediction. The results from section 3.2 indicate that the model may be applicable as close as 3 mm from the surface. However, this was never verified in section 4 as the moisture content was only measured at 11 mm.

One of the main advantages with a numerical approach is that it can be used to study the moisture variation at any depth whereas regression models usually are limited to the specific depth for which the model was derived. Consequently, a numerical model may also estimate the decay risk at different depths. In section 5 it is found that the decay rate as well as the expected service life varies significantly with depth. Moreover, the difference between the two dose models (logistic/simplified logistic) is large. Other things that can be studied using a numerical model include e.g.: other geographic effects

(latitude, altitude or closeness to water) and the influence of dimension on the service life of wooden components.

Acknowledgements

J. Niklewski acknowledges the financial support from the Wood Wisdom-Net research project Durable Timber Bridges (DuraTB). M. Fredriksson acknowledges the funding from the Swedish Research Council Formas.

[1] SS-EN 1995-2. Design of timber structures - Part 2: Bridges. Brussels: CEN (European committee for standardization); 2004.
[2] Trafikverket. Swedish recommendations for the dimensioning and design of bridges.: Trafikverket 2011; 2011.
[3] Isaksson T, Thelandersson S. Experimental investigation on the effect of detail design on wood moisture content in outdoor above ground applications. Building and Environment. 2013;59:239-49.
[4] Brischke C, Bayerbach R, Otto Rapp A. Decay-influencing factors: A basis for service life prediction of wood and wood-based products. Wood Material Science and Engineering. 2006;1:91-107.
[5] Viitanen H, Toratti T, Makkonen L, Peuhkuri R, Ojanen T, Ruokolainen L, et al. Towards modelling of decay risk of wooden materials. European Journal of Wood and Wood Products. 2010;68:303-13.
[6] Frühwald E, Brischke C, Meyer L, Isaksson T, Thelandersson S, Kavurmaci D. Durability of timber outdoor structures - Modelling performance and climate impacts. World Conference on Timber Engineering 2012: Timber Engineering Challenges and Solutions, WCTE 2012, July 15, 2012 - July 19, 2012. Auckland, New zealand: WCTE 2012 Committee; 2012. p. 295-303.
[7] Scheffer TC. Climate index for estimating potential for decay in wood structures above ground. Forest Products Journal. 1971;21:25-31.
[8] Cornick S, Alan Dalgliesh W. A moisture Index to Characterize Climates for Building Envelope Design. Journal of Thermal Envelope and Building Science. 2003;27:151-78.
[9] Van den Bulcke J, Van Acker J. Time resolved analysis of the moisture dynamics of plywood. Cost action E2008. p. 65-75.
[10] Honfi D, Mårtensson A, Thelandersson S, Kliger R. Modelling of bending creep of low- and high-temperature-dried spruce timber. Wood Science and Technology. 2014;48:23-36.
[11] Toratti T. Modelling the creep of timber beams. Rakenteiden Mekaniikka. 1992;25:12-35.
[12] Svensson S, Mårtensson A. Simulation of drying stresses in wood Part II. Convective air drying of sawn timber. Holz als Roh- und Werkstoff. 2002;60:72-80.
[13] Angst V, Malo KA. Moisture induced stresses perpendicular to the grain in glulam: review and evaluation of the relative importance of models and parameters. Holzforschung. 2010;64:609-17.
[14] Fortino S, Mirianon F, Toratti T. A 3D moisture-stress FEM analysis for time dependent problems in timber structures. Mechanics of Time-Dependent Materials. 2009;13:333-56.
[15] Nilsson L-O, Sandberg K. A new model for wetting and drying of wood end-grain - with implications for durability and service-life. The international research group on wood protection 2011: Test Methodology and Assessment, IRG/WP 2011, May 8, 2011 - May 12, 2011. Queenstown, New Zealand2011.
[16] Plumb OA, Brown CA, Olmstead BA. Experimental measurements of heat and mass transfer during convective drying of southern pine. Wood Science and Technology. 1984;18:187-204.
[17] SS-EN 335. Durability of wood and wood-based products - Use classes: definitions, applications to solid wood and wood-based products. Brussels: CEN (European committee for standardization; 2013.
[18] Fredriksson M, Wadsö L, Johansson P, Ulvcrona T. Microclimate and moisture content profile measurements in rain exposed Norway spruce (Picea abies (L.) Karst.) joints. Wood Material Science & Engineering. 2014:1-12.
[19] Tong L. Moisture diffusivities and sorption isotherms of swedish Spruce and Pine. TRITA-BYMA 1989:8. Stockholm, Sweden: The Royal Institute of Technology; 1989.
[20] Rosen H. The Influence of External Resistance on Moisture Adsorption Rates in Wood. Wood and Fiber Science. 1978;10:218-28.
[21] Wadsö L. Unsteady-state Water Vapor Adsorption in Wood: An Experimental Study. Wood and Fiber Science. 1994;26:36-50.
[22] Frandsen HL, Damkilde L, Svensson S. A revised multi-Fickian moisture transport model to describe non-Fickian effects in wood. Holzforschung. 2007;61:563-72.

[23] Krabbenhoft K, Damkilde L. A model for non-Fickian moisture transfer in wood. Materials and Structures. 2004;37:615-22.
[24] Häglund M. Moisture content penetration in wood elements under varying boundary conditions. Wood Sci Technolog. 2007;41:477-90.
[25] Simpson WT. Determination and use of moisture diffusion coefficient to characterize drying of northern red oak (Quercus rubra). Wood Sci Technolog. 1993;27:409-20.
[26] Koponen H. Dependences of moisture diffusion coefficients of wood and wooden panels on moisture content and wood properties. Paperi ja puu. 1984;66:740-5.
[27] Nilsson L. Fukttransportegenskaper hos trä och träbaserade skivor. Chalmers Tekniska Högskola: Avdelningen för Byggnadsmaterial; 1988.
[28] Angst-Nicollier V. Moisture induced stresses perpendicular to the grain in glulam: Review and evaluation of the relative importance of models and parameters. Holzforschung. 2010;64.
[29] Koponen H. Dependences of moisture transfer coefficients on moisture diffusion coefficients and wood properties. Paperi ja puu. 1985;67:363-8.
[30] Time B. Hygroscopic moisture, transport in wood: Norwegian University of Science and Technology; 1998.
[31] Miner MA. Cumulative damage in fatigue. Journal of Applied Mechanics. 1945;67:A159-A64.
[32] Isaksson T, Brischke C, Thelandersson S. Development of decay performance models for outdoor timber structures. Materials and Structures/Materiaux et Constructions. 2013;46:1209-25.
[33] Fredriksson M. Moisture conditions in rain exposed wood joints - Experimental methods and laboratory measurements. Lund: Lunds University; 2013.
[34] COMSOL Multiphysics. Version 4.4. 2013.
[35] Fredriksson M, Wadso L, Johansson P. Small resistive wood moisture sensors: a method for moisture content determination in wood structures. European Journal of Wood and Wood Products. 2013;71:515-24.
[36] Derome D, Zillig W, Carmeliet J. Variation of measured cross-sectional cell dimensions and calculated water vapor permeability across a single growth ring of spruce wood. Wood Science and Technology. 2012;46:827-40.
[37] SMHI. Swedish Meteorological and Hydrological Institute; 2015.
[38] Hjort S. Full-scale method for testing moisture conditions in painted wood paneling. JCT, Journal of coatings technology. 1996;68:31-9.
[39] Fredriksson M, Wadsö L, Johansson P. Methods for determination of duration of surface moisture and presence of water in gaps in wood joints. Wood Science and Technology. 2013;47:913-24.
[40] Meteonorm. [Computer Software] V7.1.3.19872. 2014.